Solution Conformation of the Antitumor Antibiotic Chromomycin A_3 Determined by Two-Dimensional NMR Spectroscopy†

Michal Kam,‡ Richard H. Shafer,§ and Elisha Berman*,‡

Department of Organic Chemistry, The Weizmann Institute of Science, Rehovot 76100, Israel, and Department of Pharmaceutical Chemistry, School of Pharmacy, University of California, San Francisco, California 94143

Received August 19, 1987; Revised Manuscript Received January 7, 1988

ABSTRACT: A conformational analysis and a complete assignment of the nonexchangeable proton resonances of chromomycin A_3, dechromose-A chromomycin A_3, and deacetylchromose-B chromomycin A_3 were carried out in organic solvents. The resulting conformation in methanol has the three side chains of chromomycin A_3 fully extended, away from one another and from the aglycon. In dichloromethane on the other hand, the drug was shown to adopt a highly compact conformation in which most of the 26 oxygen atoms in the molecule point out toward the solvent. The two carbohydrate side chains extend parallel to each other on the same side of the aglycon. Two intramolecular nuclear Overhauser enhancement contacts have been observed between different sugar units on these side chains, indicating close proximity for these moieties. In addition, the aliphatic side chain is folded toward the aglycon, parallel to the two oligosaccharide side chains. The overall conformation has a wedge-like shape with the two phenoxy groups exposed at the pointed edge. The presence of some exchange cross-peaks in the NOESY spectra suggests the presence of intramolecular hydrogen bonds that probably help to maintain the compact conformation. The derivatives of chromomycin A_3 have qualitatively similar conformations, though their respective conformations are not as compact as the parent drug. The significance of these results is discussed in terms of a model of chromomycin A_3 binding to DNA in the major groove.

Chromomycin A_3 (CRA)[1] is an antitumor antibiotic that belongs to the aureolic acid group (Remers, 1979) and is composed of chromomycinone, two oligosaccharide side chains which carry a total of five 2,6-dideoxyhexopyranoses (Miyamoto et al., 1967), and a heavily substituted aliphatic side chain (Chart I). The molecule has 26 oxygen atoms with a great potential for intramolecular hydrogen bonding, but at the same time, the molecule possesses hydrophobic regions (e.g., the polyaromatic aglycon).

Following the initial work on the structure of chromomycin A_3 (Miyamoto et al., 1967), the complete stereochemistry of chromomycin A_3 was established by Thiem and Meyer (1979) using NMR spectroscopy. They have provided assignments for nearly all the proton and carbon resonances of CRA and related aureolic acids (Thiem & Meyer, 1979, 1981). Using 2D NMR spectroscopy, we have confirmed most of the previous assignments and provided a complete proton assignment for CRA. We have also studied two other derivatives: CRA-B, which does not contain the 2,6-dideoxy-4-*O*-methyl-α-D-*lyxo*-hexopyranose unit (sugar B in Chart I), and CRA-OAc, for which the acetate group of sugar unit E (4-*O*-acetyl-2,6-dideoxy-3-*C*-methyl-α-L-*arabino*-hexopyranose) is missing. Using 2D nuclear Overhauser enhancement NMR experiments (NOESY) at 270 and 500 MHz, we were able to obtain the solution conformation of CRA in dichloromethane and in methanol, respectively. The high aggregation tendency exhibited by CRA at all pH values prevented the use of water as solvent at the millimolar concentrations required for the NMR experiments. Results were compared with the recently reported conformation of CRA when bound to DNA hexamer duplex (Keniry et al., 1987).

Materials and Methods

Chromomycin A_3 (>95% purity) was obtained from Sigma Chemical Co., St. Louis, MO. Silica gel (230–400 mesh) for column chromatography was purchased from Merck Co., Darmstadt, FRG. All other chemicals used were of reagent-grade quality.

Preparation of the CRA Hydrolysis Products. A modified hydrolysis procedure (Miyamoto et al., 1967) was employed in order to minimize the appearance of the more advanced, unwanted, hydrolysis products. The drug (10–20 mg) was dissolved in 3 mL of acetic acid/water (1:1 v/v), and the reaction was carried out at 45 °C for 5.5 h with no stirring. The progress of the reaction was monitored by TLC (silica gel), eluted by 3% oxalic acid in ethyl acetate and developed by the vaniline reagent. The reaction was quenched by the addition of 3 volumes of distilled water to the reaction, followed by extraction with ethyl acetate. The organic layer was washed successively with water, saturated sodium bicarbonate, and water again until pH 6 was obtained. The washed organic layer was dried on magnesium sulfate, filtered, and evaporated to dryness under reduced pressure at room temperature. The solid residue was separated into its components by flash-chromatography techniques. The column was packed with silica gel, and the eluting solvent was 3% oxalic acid in ethyl acetate. Fractions (2 mL) were collected and examined by the TLC technique as described above. The two major spots that were observed corresponded to the starting material and to its first hydrolysis product from which chromose-A was

† This work supported by a grant from the U.S.–Israel Binational Foundation.

‡ The Weizmann Institute of Science.

§ University of California.

[1] Abbreviations: CRA, chromomycin A_3; CRA-B, dechromose-A chromomycin A_3; CRA-OAc, deacetylchromose-B chromomycin A_3; 2D, two dimensional; NOE, nuclear Overhauser enhancement; NOESY, ^{1}H two-dimensional NOE correlation NMR in absolute absorption mode; TLC, thin-layer chromatography; DNA, deoxyribonucleic acid; COSY, ^{1}H homonuclear *J*-correlation NMR; relayed COSY, ^{1}H magnetization-transfer homonuclear *J*-correlation NMR; CD, circular dichroism spectroscopy; SDS, sodium dodecyl sulfate.

0006-2960/88/0427-3581$01.50/0

Chart I: Structure of Chromomycin A_3 (Top) and a Schematic Drawing of the Solution Conformation of Chromomycin A_3 in Dichloromethane (Bottom)[a]

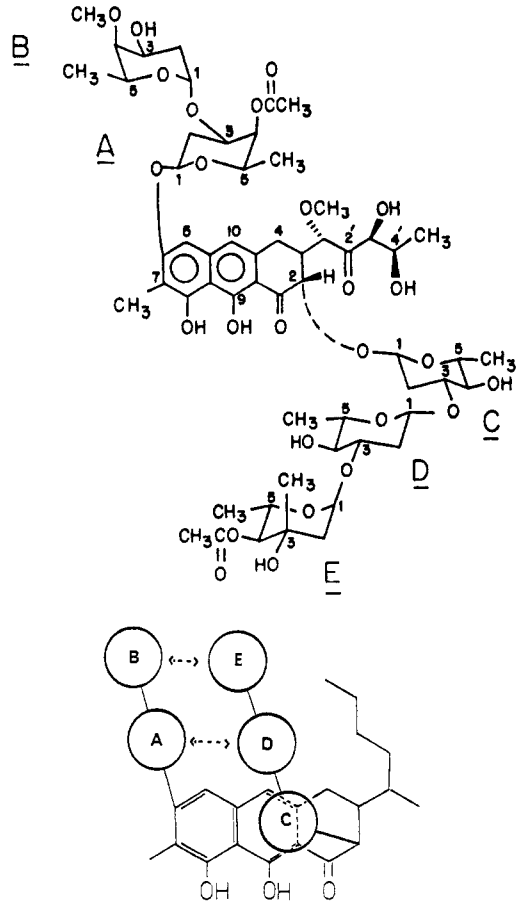

[a] The double-headed arrows indicate close proximity between respective sugar units.

removed (CRA-B). Fractions showing the same spot on the TLC plate were pooled and washed with water followed by saturated sodium bicarbonate solution and finally with water again. The starting material was recycled and used for further production of CRA-B in order to maximize the yield.

The deacetylchromose-B chromomycin A_3, CRA-OAc, was obtained according to a method similar to the published procedure (Miyamoto et al., 1967), and it was separated from the starting material on the same column described above.

NMR of CRA and Derivatives in Dichloromethane. The spectra were recorded on a Bruker WH-270 spectrometer operating at 270 MHz for protons. Samples of vacuum-dried chromomycin A_3 and its derivatives were dissolved in dry dichloromethane-d_2 (10–15 mg/mL) and transferred to a 5-mm NMR tube, and their spectra were recorded at 27 °C. Spectra were collected on an Aspect 2000 computer with a spectral window of 2809 Hz, an 85° pulse width (10 μs), 16384 data points, and a repetition rate of 3 s. After the data were zero-filled, a Gaussian window function was used to enhance spectral resolution.

COSY spectra were recorded with the standard two-pulse sequence provided by Bruker. Spectral window of 1695 Hz was used with a 230 × 1024 data matrix and 2-s delay between each of the 112 transients accumulated for each of the t_1 values. The data were zero-filled to yield a final matrix of 512 × 1024 and processed with a shifted square sine bell function ($\pi/16$), followed by symmetrization of the spectrum. Relayed COSY spectra were recorded with the same spectral parameters and the appropriate pulse sequence for a two-step magnetization transfer relay (the transfer delay was set to 0.06 s). NOESY spectra were recorded under similar spectral conditions with a phase-cycled three-pulse sequence to remove most of the possible artifacts from the spectrum, and additionally, the mixing delay was randomly varied by ±20 ms to cancel zero-quantum contributions. Spectra with seven different mixing times (0.1, 0.2, 0.4, 0.6, 0.8, and 1.4 s) were recorded to allow for the optimization of the NOE transfer conditions for the various cross-peaks.

NMR of CRA in Methanol. Spectra were recorded on a Bruker AM-500 spectrometer operating at 500 MHz for protons. The concentration of the CRA in methanol-d_4 did not exceed 2 mM to avoid drug self-aggregation. Spectra were collected on an Aspect 3000 computer with a spectral window of 3600 Hz, an 85° pulse width (7 μs), 32768 data points, and a repetition rate of 4.5 s. After the data were zero-filled, a Gaussian window function was used to enhance spectral resolution.

Phase-sensitive COSY spectra were recorded with the pulse sequence provided by Bruker. A spectral window of 3600 Hz was used with a data matrix of 480 × 2048 and a 2-s delay between each of the 64 transients accumulated for each of the t_1 values. The data were zero-filled to yield a final matrix of 2048 × 2048 and processed with a shifted square sine bell function ($\pi/8$), followed by symmetrization of the spectrum. Relayed COSY spectra were recorded with the same spectral parameters and the appropriate pulse sequence for a two-step magnetization transfer relay (the transfer delay was set to 0.06 s). Phase-sensitive NOESY spectra were recorded under the same conditions but with irradiation of the water resonance at 4.9 ppm to enable the observation of resonances otherwise overlapped by the solvent peak. Three mixing times were recorded (0.2, 0.4, and 0.6 s) at two temperature (27 and 15 °C); the lower temperature was chosen to enhance the observed intensity of the NOE cross-peaks.

Results and Discussion

Chemical Shift Assignments. The published ^{1}H NMR chemical shift assignments for chromomycin A_3 (Thiem & Meyer, 1979) did not include specific assignments for the two methoxy and the two acetoxy methyl groups of chromomycin A_3. We have obtained unambiguous assignments for these resonances by comparing the spectrum of CRA (Figure 1) with that of CRA-B. Removing sugar unit B from the chromomycin A_3 molecule caused one of the methoxy methyl resonances to disappear from the spectrum, as well as a change in the chemical shift of the acetoxy methyl group of sugar unit A. The chemical shifts of the other methyl resonances in the spectrum of CRA-B were not expected to be influenced.

Careful examination of the ^{1}H NMR spectra of CRA and CRA-B in dichloromethane has led us to reexamine some of the previously reported proton assignments for chromomycin A_3 (Thiem & Meyer, 1979). 2D NMR spectroscopy was used to obtain resonance assignments for CRA, CRA-B, and CRA-OAc, which were reconfirmed by direct comparison with the chemical shift data obtained for the corresponding data obtained for CRA in methanol (Table I). Few proton reassignments had to be made, most important of which being the interchange of the H1 and the two H2 protons of sugar B with their corresponding protons on sugar unit E.

The hydroxyl proton resonances were not observed in methanol because of exchange with the deuteriated protic solvent. In dichloromethane these resonances exhibit some variation in the value of the chemical shifts and the magnitude of the observed line widths depending on the humidity level of the solvent. In wet dichloromethane solutions the hydroxyl

Table I: ^1H NMR Chemical Shifts for Chromomycin A_3 (CRA), Its Monodeacetyl Derivative (CRA-OAc), and the First Hydrolysis Product (CRA-B)[a]

	aglycon[b]									
	2	3	4a	4e	5	10	1′	3′	4′	5′
CRA	4.73	2.61	3.10	2.68	6.66	6.78	4.69	4.23	4.35	1.36
CRA[c]	4.71	2.805	2.995	2.665	6.750	6.820	4.870	4.160	4.220	1.240
CRA-OAc	4.71	2.59	3.08	2.66	6.65	6.78	4.70	4.24	4.33	1.35
CRA-B	4.73	2.62	3.10	2.69	6.69	6.81	4.70	4.24	4.35	1.36

	A							
	1	2a	2e	3	4	5	6	OAc-4
CRA	5.25	2.15	2.09	3.99	5.16	3.82	1.24	2.16
CRA[c]	5.390	2.04	2.08	4.090	5.180	3.905	1.210	2.145
CRA-OAc	5.24	2.13	2.07	3.99	5.14	3.82	1.25	2.15
CRA-B	5.25	2.18	2.02	4.02	5.05	3.84	1.26	2.19

	B[d]							
	1	2a	2e	3	4	5	6	OMe-4
CRA	5.08	1.68	1.70	3.91	3.19	3.87	1.27	3.56
CRA[c]	5.095	1.860	1.605	3.960	3.220	3.935	1.220	3.560
CRA-OAc	5.09	1.67	1.70	3.92	3.19	3.86	1.35	3.56

	C						
	1	2a	2e	3	4	5	6
CRA	5.10	1.68	2.49	3.60	3.07	3.30	1.33
CRA[c]	5.115	1.595	2.590	3.725*	3.025	3.32	1.335
CRA-OAc	5.11	1.68	2.48	3.60	3.05	3.30	1.33
CRA-B	5.10	1.67	2.49	3.60	3.07	3.30	1.33

	D						
	1	2a	2e	3	4	5	6
CRA	4.61	1.63	2.28	3.52	3.08	3.38	1.35
CRA[c]	4.72	1.470	2.340	3.560*	3.050	3.38	1.325
CRA-OAc	4.61	1.62	2.26	3.49	3.08	3.37	1.36
CRA-B	4.61	1.62	2.28	3.50	3.10	3.38	1.35

	E							
	1	2a	2e	3	4	5	6	CH_3	OAc-4
CRA	5.03	2.01	2.00		4.60	3.98	1.22	1.36	2.12
CRA[c]	5.040	1.930[+]	1.935[+]		4.670	4.095	1.115	1.435	2.090
CRA-OAc	4.97	1.91	2.00		3.25	3.82	1.31		
CRA-B	5.03	2.01	2.00		4.60	3.98	1.22	1.36	2.12

[a] A 15 mM solution in CD_2Cl_2 at 30 °C; referenced to $CDHCl_2$ signal at 5.32 ppm. Chemical shifts were derived from the 1D and 2D NMR spectra taken at 270 and 500 MHz. (*) Assignments were confirmed by decoupling experiments. (+) Assignment may be interchanged. [b] Other signals were 2.18, 2.18, and 2.18 ppm (CH_3-7), 3.50, 3.50, and 3.50 ppm (OCH_3-1′), 3.58 and 3.58 ppm (OH-3′), and 9.81, 9.81, and 9.83 ppm (OH-8) for CRA, CRA-OAc, and CRA-B, respectively. [c] Data for chromomycin A_3 in methanol taken at 500 MHz. Other resonances: 2.155 ppm (OCH_3-7); 3.425 ppm (OCH_3-1′). [d] This sugar unit is missing from the structure of CRA-B.

proton resonances were not observed at all because these protons exchange with the residual water in the solvent, except for the C3′ hydroxyl proton which did not exchange. The C3′ hydroxyl proton has a clear coupling to H3′ as indicated by a COSY cross-peak to H3′ (Figure 2), and so it is localized on the O3′ atom, rather than forming an intramolecular hydrogen bond (e.g., to the carbonyl oxygen of C2′). It is also likely that the molecule adopts a conformation in which the C3′ hydroxyl group has limited solvent accessibility.

The chemical shifts of the protons from either the aglycon or the trisaccharide side chain are not affected by the removal of sugar unit B from CRA. The chemical shift changes for the sugar unit A protons are unexpectedly small, the largest change being for the H4 proton (0.11 ppm) and a small downfield shift for H3 (0.03 ppm). The downfield shift of H3 is rather unexpected since an upfield shift (>0.15 ppm) is normally associated with the proton attached to the deglycosylation site. The axial orientation of the anomeric oxygen forces the sugar B ring into an almost perpendicular position relative to sugar A. Nonbonding interactions are, thus, expected to modify the normal values of the glycosylation substituent chemical shifts. As expected, deacetylation of C4 of sugar E resulted in a large upfield chemical shift change for H4 (1.35 ppm), H5 (0.16 ppm), and H1 (0.06 ppm). Small or no chemical shift changes were observed for protons outside ring E. The upfield shift of the anomeric proton of sugar E is also accompanied by a change in magnitude of the three-bond coupling constant to one of the H2 protons. In CRA (and CRA-B) we find $^3J_{H1,H2e} = 2.2$ Hz, and in the monodeacetyl derivative it is only 1.6 Hz (Figure 3). It is clearly a reflection of the conformational strain in the sugar E ring brought about by the additional methyl group at the C3 position. Such a methyl group destabilizes the ring chair conformation in which the C6 methyl group normally occupies an equatorial position. The change in coupling constant is not sufficient to indicate appreciable deviation in the predicted chair conformation for sugar E. The small magnitude of the vicinal couplings between the anomeric proton and the two H2 protons in sugar unit E clearly point to an equatorial orientation of the anomeric proton.

Chemical shift differences of up to 0.2 ppm were observed for corresponding resonances of CRA in methanol relative to dichloromethane solution. These changes reflect both solvent and concentration dependence of the chemical shifts. It is supported by the fact that essentially identical magnitudes of corresponding coupling constants were observed.

Solution Conformation of Chromomycin in Dichloromethane. Following the assignment of the nonexchangeable

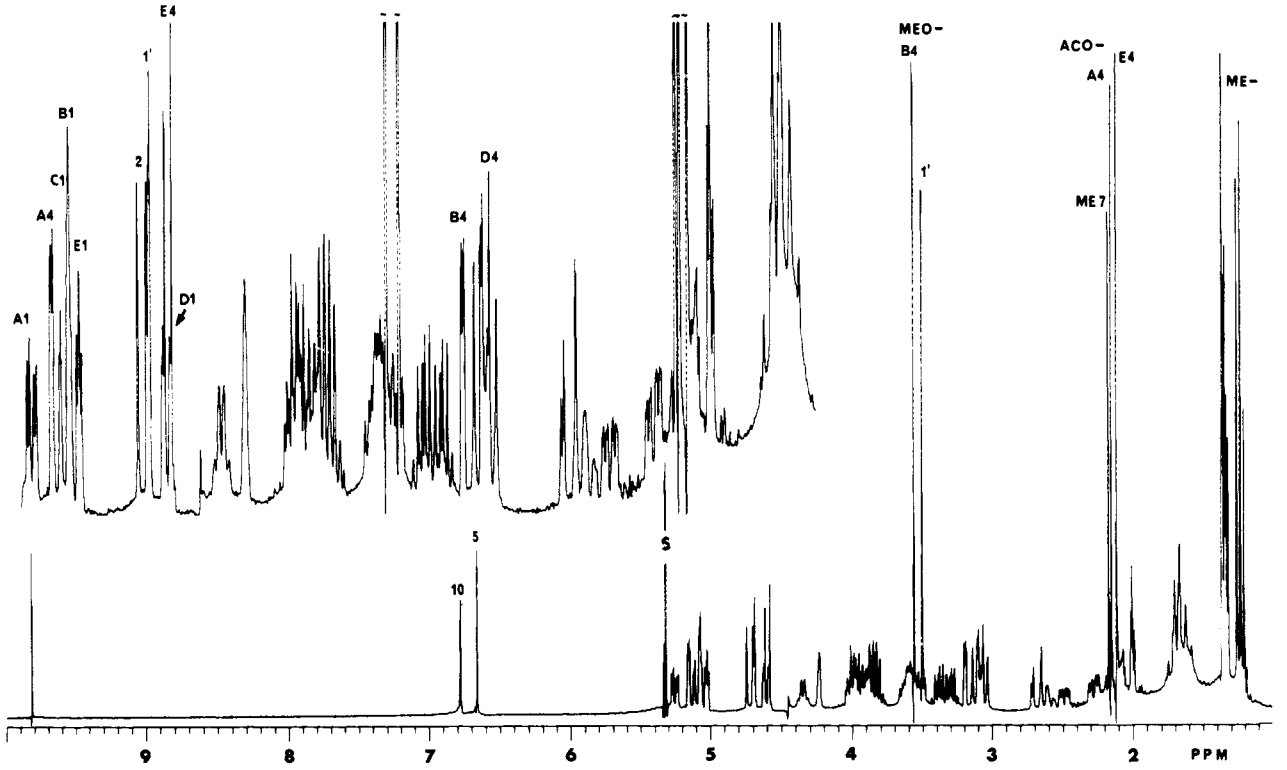

FIGURE 1: A 270-MHz ^{1}H NMR spectrum of a 10 mM solution of chromomycin A_3 in dichloromethane. Inset shows an expanded region of the spectrum (5.3–1.5 ppm) that includes most of the proton resonances.

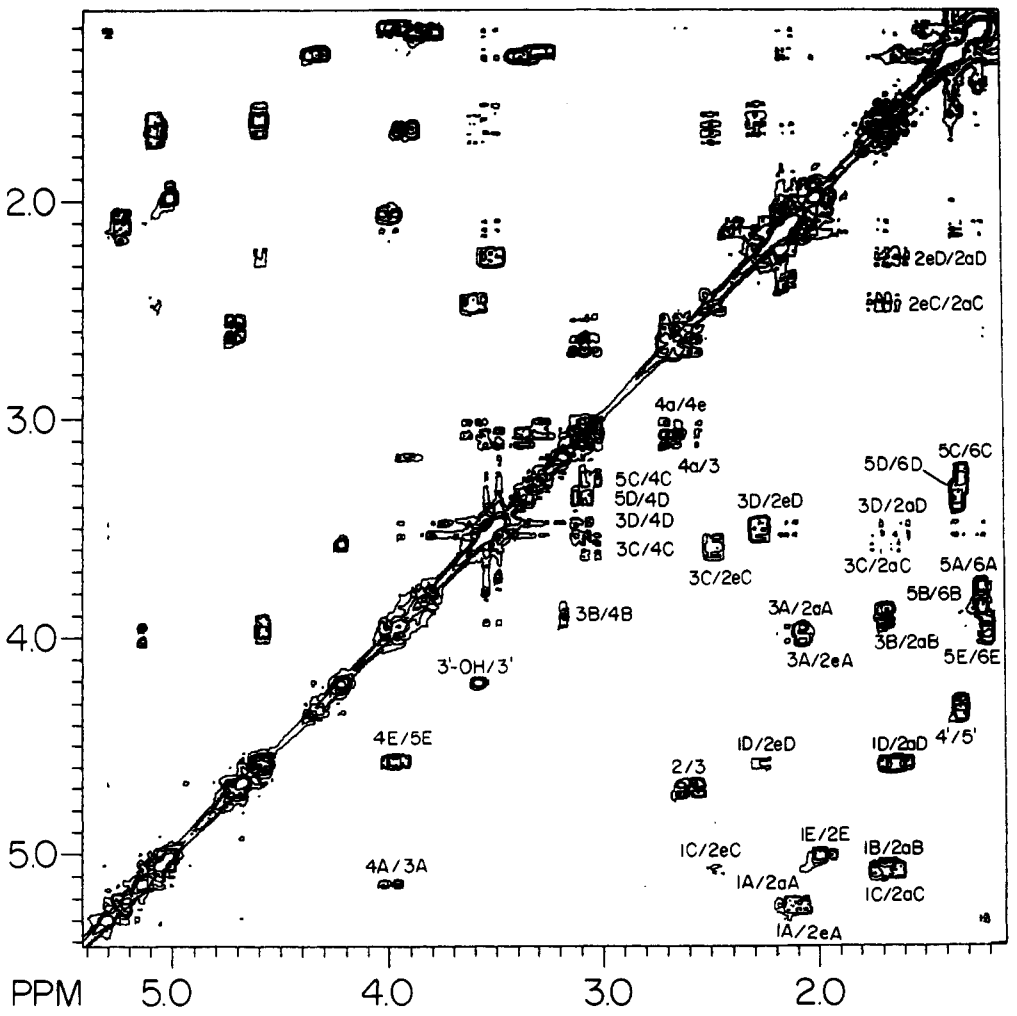

FIGURE 2: A 270-MHz ^{1}H COSY map of chromomycin A_3 (CRA) in dichloromethane showing the upfield spectral region. Assignments are given for cross-peaks below the diagonal, and the corresponding chemical shifts are listed in Table I.

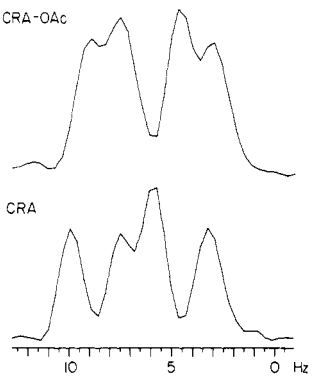

FIGURE 3: Expanded anomeric proton (H1) resonance multiplets of sugar unit E in chromomycin A_3 (CRA) (bottom) and its monodeacetyl derivative (CRA-OAc) (top) taken under the same conditions showing the differences in the apparent vicinal coupling constants to the two H2 protons.

Table II: NOE Contacts Observed for Chromomycin A_3 (CRA) and Its Two Derivatives CRA-B and CRA-OAc[a]

NOE contacts	CRA	CRA-B	CRA-OAc
(1) 1′ → 1′-OMe	++	++	++
(2) 2 → 1′-OMe	++	++	+
(3) 5 → 1A	+	++	+
(4) 4A → 4D	++		+
(5) 4B → 4B-OMe	++		++
(6) 4B → 1E	++		
(7) 1E → 2E	++	+	*b*
(8) 1E → 4E			+

[a] Only strong (++) and intermediate (+) NOE contacts are indicated. These peaks consistently appeared in spectra taken at various mixing times and did not change or reduced in intensity upon doping the sample with D_2O. [b] Only a weak cross-peak was observed.

protons of CRA, NOESY experiments with varying mixing delays (0.1–1.4 s) were performed. At the optimum mixing time (0.6 s), many cross-peaks were detected mostly with rather low intensity, but a number of more intense cross-peaks were clearly discerned in the spectrum, and these are displayed in Figure 4 by plotting at the appropriate contour levels.

The stronger cross-peaks include exchange peaks between the residual water and some of the hydroxyl proton resonances (marked e in Figure 4) and intramolecular hydrogen-bonding exchange cross-peaks (marked d in Figure 4). Both types of exchange cross-peaks disappear slowly upon doping the sample with deuteriated water. Other cross-peaks are identified as pure NOE contacts (marked a in Figure 4) associated with protons belonging to the three side chains of CRA. Unlike large molecules such as proteins and DNA segments, small molecules tend to establish conformational equilibrium between a number of possible conformations. Therefore, the dominant solution conformation of CRA will be the only one to be associated with the strong NOE contacts while it is expected that some of the weaker NOE contacts observed in the spectrum actually arise from NOE contributions that originate with the minor conformation. This ambiguity in the origin of the lower intensity NOE contacts prevents their use as primary data in any subsequent conformational analysis. Only firmly assigned strong NOE contacts (Table II) were used for the interpretation of the data in terms of the three-dimensional conformation of CRA. Analysis of these NOE contacts together with the coupling constant information (Thiem & Meyer, 1979) yielded a unique, well-defined conformation for the drug (shown in Chart I).

The interproton distances for some of the pairs of protons that give rise to the NOE contacts listed in Table II can be estimated as these protons are located at a fixed distance from each other. Thus, the NOE entries 1 and 5 correspond to interproton distance in the range of 0.25–0.3 nm, and entry 7 in Table II corresponds with a distance of 0.25 nm. By comparison of the relative cross-peak intensities, we have estimated the interproton distances between two protons that lay across the two sugar side chains (entries 4 and 6 in Table II) to be around 0.3 nm and not more than 0.4 nm. Likewise, the interproton distance in the case of entry 2 was taken to be about 0.3 nm, whereas entry 3 corresponds to a slightly longer distance. On this basis, we built a molecular model representing the conformation of the chromomycin A_3 molecule in solution. This model was visually optimized to include as many of the observed small NOE cross-peaks as possible (data not shown). At the same time, we required that no two protons will come close enough in space to have yielded strong NOE contacts otherwise not observed in the spectrum. The final three-dimensional conformation for CRA is rather unexpectedly compact with most of the oxygen groups exposed to the solvent. The carbohydrate side chains are extended, parallel to each other, on the same side of the aglycon plane, with sugar units B and E and sugar units A and D close in space to each other (Figure 5A). The aliphatic side chain is folded toward the aglycon from the same side as the other two side chains, forming a well-defined hydrophobic pocket enclosed by the side chains and the aglycon. Sideways projection of the structure has a wedged-slab appearance with its thin face being some 1.0–1.2 nm across and with the hydrophilic phenoxy groups at its tip (Figure 5B). The overall structure is held together by a number of intramolecular hydrogen bonds, as indicated by the presence of strong exchange cross-peaks in the spectrum (marked d in Figure 4). Additional energy is gained by the minimization of the hydrophobic interactions. The two terminal sugars (units B and E) have their anomeric oxygen in an axial orientation (Thiem & Meyer, 1979); therefore, these sugars must adopt unique conformations in order to reduce the strong nonbonded interactions with the penultimate sugar residues. This constraint may also contribute to the final conformation of the drug.

By use of the corresponding NOE data (Table II), similar conformations were constructed for the two chromomycin A_3 derivatives. The conformation of CRA is basically retained in these derivatives, but with an increased separation between the side chains. The NOE contact between sugar unit E and sugar unit B (Table II, entry 6) has disappeared from the NOESY spectrum of the deacetylated sugar E derivative (CRA-OAc), while the other NOE contacts have considerably reduced relative intensities. The two important interresidue NOE contacts between sugars B and E and between units A and D (Table II, entries 4 and 6) could not be detected in the spectrum of CRA-B. Therefore, in the case of CRA-OAc the two oligosaccharide side chains are further apart from each other relative to their positions in the CRA conformation, and the separation between these two side chains is even greater for CRA-B which does not have sugar B.

Solution Conformation of Chromomycin in Methanol. At 27 °C weak negative NOE cross-peaks were observed in the phase-sensitive NOESY spectra of CRA. The relative signal intensities of the NOESY cross-peaks were improved by repeating the experiments at 15 °C. The observed cross-peaks were grouped into two classes according to their origin (Table III). The first type of NOE contacts arises from proximate protons that are fixed in space relative to each other (e.g., on the same sugar ring). The second type of NOE contacts represents proximate protons which are connected through a flexible segment of the molecule (e.g., on two different sugar

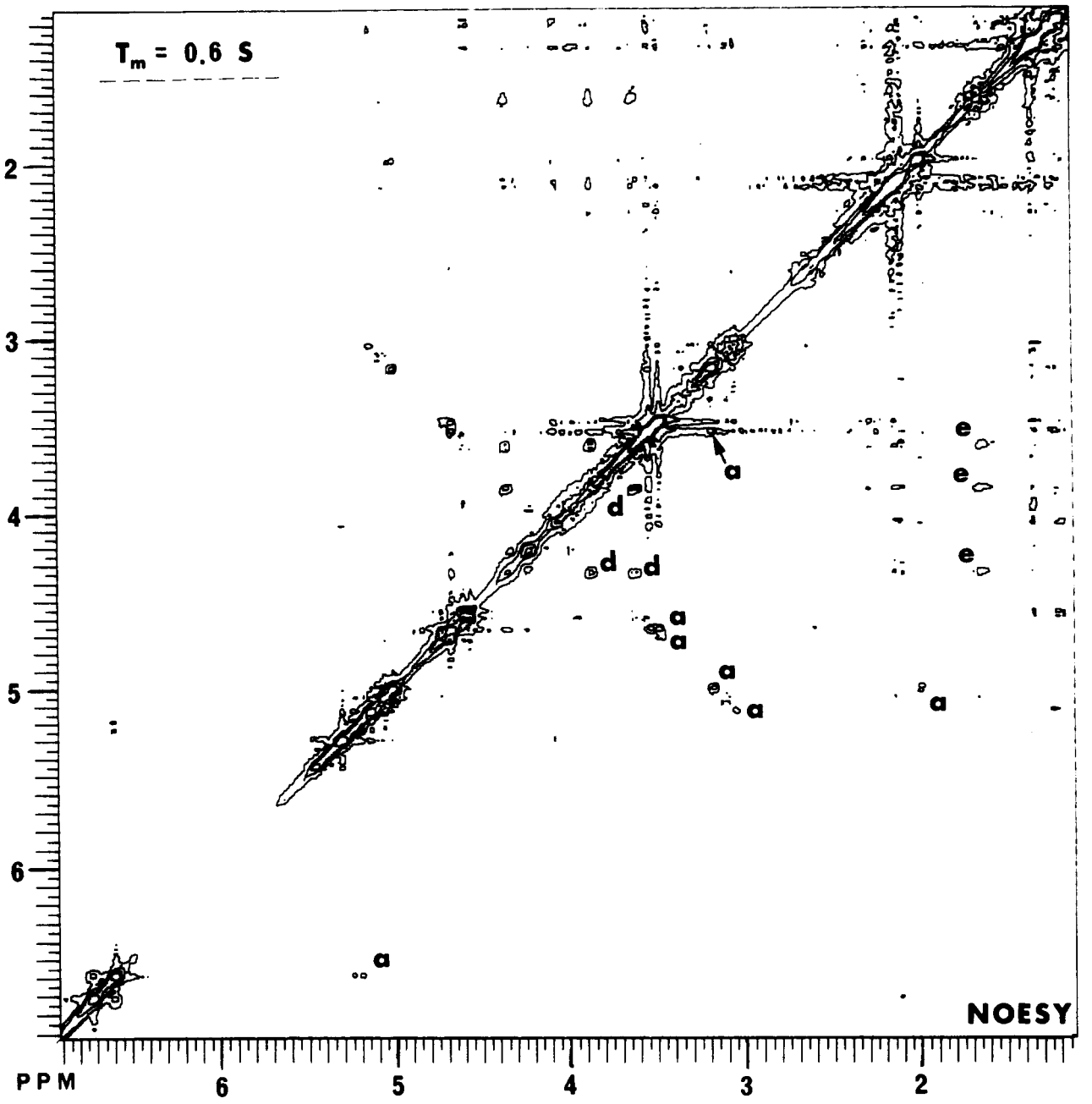

FIGURE 4: A 270-MHz ^{1}H NOESY map of chromomycin A_3 in dichloromethane, showing the strong cross-peaks in the spectrum. (a) NOE contacts; (d) intramolecular hydrogen-bond exchange cross-peaks; (e) exchange cross-peaks with the residual water resonance.

units). Unlike the case of CRA in dichloromethane, only one conformation of CRA was observed. By analogy to the case of CRA in dichloromethane, only the constraining type of NOE contacts (Table III) was used to arrive at a molecular model for the conformation of CRA in methanol. In that conformation all three side chains extend away from each other and from the aromatic core of the aglycon (Figure 6). It is an averaged solution conformation for CRA which is very similar to the energy-minimized conformation calculated for CRA (B. Meyer, personal communication). The choice of methanol as solvent ensures that no intramolecular hydrogen bonds will be formed; as a result, the hydrophobic interactions alone are insufficient to stabilize a folded conformation. Instead, the hydrophobic interactions apparently induce stacking of the flat CRA molecules as observed at higher concentrations and in water (Weinberger et al., 1988).

Conclusions

Analysis of the NOE contacts indicated that a folded conformation is predominant for CRA in dichloromethane, while a fully extended conformation was observed for CRA dissolved in methanol. The folded conformation of the drug is not predicted by energy minimization calculations performed with the primary not predicted by energy minimization calculations performed with the primary structure data alone (B. Meyer, personal communication). The folded solution conformation of CRA is determined to a large degree from the presence of an uneven distribution of hydrophilic and hydrophobic regions in the molecule. In principle, the folding of the three side chains to one side of the polyaromatic aglycon, with consequent formation of a hydrophobic pocket, should be enhanced in more polar solvents as a result of stronger hydrophobic interactions. This assumption is also supported by findings from absorption and CD spectroscopic studies of very dilute CRA solutions in various solvents (Weinberger et al., 1988). Several observed spectral features were enhanced by going from dichloromethane solution through ethanol to water solution. These were distinctly different from those observed for the drug

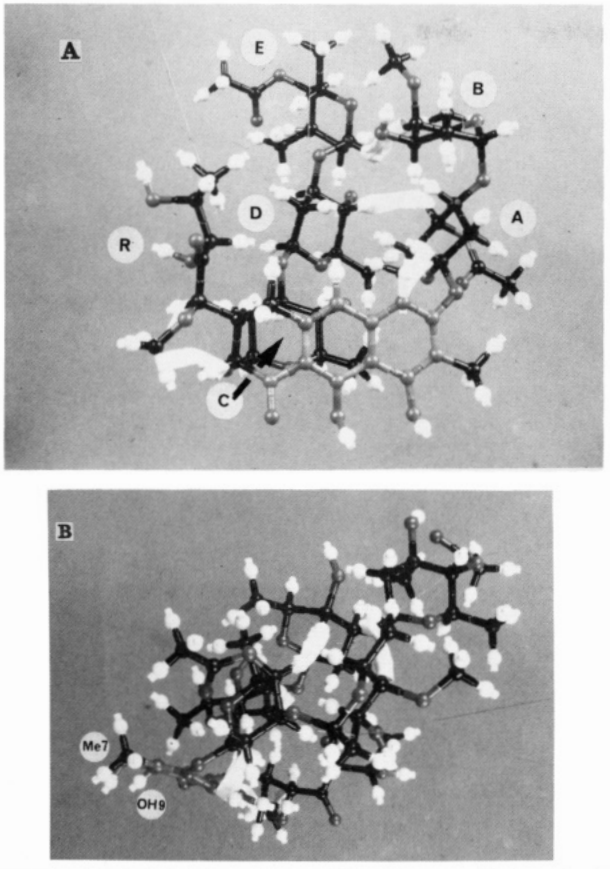

FIGURE 5: (A) Broad-side projection of the chromomycin A_3 molecule showing the orientation of the three side chains relative to the aglycon. The letters A–E corresponds with the sugar notation given in Chart I, and R denotes the aliphatic side chain. (B) Side projection of the chromomycin A_3 molecule in dichloromethane showing the wedge-like conformation with the hydrophilic part of the aglycon at its tip. Functional groups that are implicated as buried deep inside the major groove in the drug–DNA complex are identified. Strips connecting parts of the molecule correspond to some of the observed NOE contacts.

Table III: NOE Observed for Chromomycin A_3 in Methanol at 15 °C[a]

fixed-distance NOE				constraining NOE	
1	2/4a	17	B1/B2e	1	1′/3
2	3/4e	18	B1/B2a	2	1′/3′
3	3/4a	19	B2a/B2e	3	1′/4′
4	4a/4e	20	B4/B5	4	3′/5′
5	4a/10 (w)	21	B4/BOMe	5	3′/3
6	4e/10	22	B6/BOMe	6	5/A1
7	5/10	23	C1/C3	7	5/A5 (w)
8	1′/1′-OMe	24	C1/C2e	8	B1/A3
9	3′/4′	25	C1/C5	9	B1/A4
10	A1/A3	26	C2a/C2e	10	C1/2
11	A1/A5	27	C2a/C4 (w)	11	C3/2 (w)
12	A3/A4	28	C4/C5	12	E1/D2e (w)
13	A3/A5	29	C4/C6		
14	A4/A5	30	D2a/D2e		
15	A4/A6	31	D4/D5		
16	A5/A6	32	E1/E2a,E2e		

[a] Taken from the phase-sensitive NOESY spectrum at 500 MHz (0.45-s mixing time) with irradiation of the HDO signal at 4.93 ppm. (w) denotes weak cross-peak.

solutions in nonpolar organic solvents or in 10% SDS aqueous solution. Polar solvents are generally capable of forming solvent–solute hydrogen bonds which directly compete with the formation of intramolecular hydrogen bonds. Use of methanol prevented the formation of intramolecular hydrogen bonds and served to destabilize the folded conformation relative

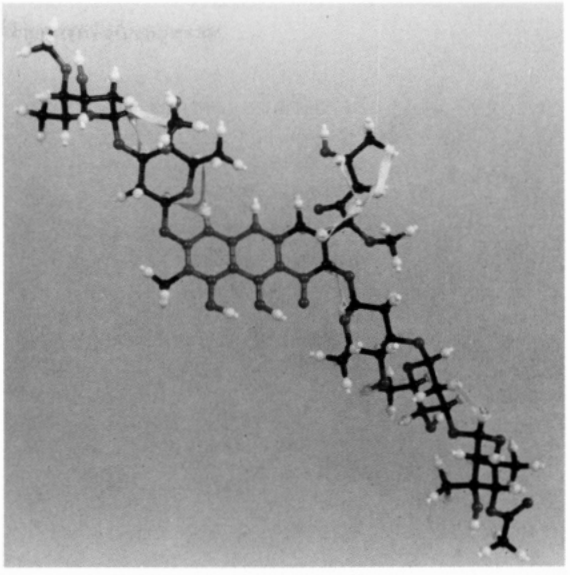

FIGURE 6: Broad-side projection of the chromomycin A_3 molecule dissolved in methanol showing the relative orientation of the side chains. Strips connecting parts of the molecule correspond to some of the observed NOE contacts.

to the fully extended conformation of CRA. The relative populations of the conformations of CRA clearly depend on the interplay of these opposing forces, and the final outcome will determine the predominant conformation in a given solvent. The net stabilization energy must be very small indeed for the CRA to have such a labile preferred conformation. At the same times it also offers a distinct advantage for it will ensure that CRA will adopt the preferred conformation, making itself recognizable while possessing the conformational flexibility needed for its receptor interactions.

We could not firmly assign the hydroxyl protons involved in the formation of the intramolecular hydrogen bonding because of the chemical shift variability typically observed for such protons. A partial answer may be provided from energy-minimization calculations that will point to likely hydrogen binding sites. It is also unfortunate that NMR methods could not be used to determine the solution conformation of chromomycin A_3 in water because of an extensive aggregation of the drug.

Though comparison between the free drug conformation and its bound state conformation cannot be made directly, it is interesting that two important NOE contacts were observed both for the free drug dissolved in dichloromethane and for the DNA-bound CRA (Keniry et al., 1987). These contacts (Table II, entries 2 and 3) are important because they fix the orientation of the corresponding side chains. In the drug–DNA complex, the CRA molecule has its aliphatic side chain folded in the direction of the aglycon in much the same way as found for the free state. The orientation of sugar unit A of the disaccharide side chains is the same in both the free and the complexed conformations of the drug. On the other hand, sugar unit B is folded back toward the aglycon when the drug is complexed rather than extended as found for the free chromomycin A_3. Upon binding to the major groove of the DNA, a number of water molecules are likely to be displaced from the hydration shell of the drug, thus creating a favorable environment for the formation of intramolecular hydrogen bonds. These may serve to stabilize a folded conformation for CRA similar to that found for the free drug in dichloromethane. The pointed end of this conformation includes both the hydrophilic phenoxy groups and the aromatic methyl group, which were shown to be very close to the DNA base

protons at the DNA major groove (Keniry et al., 1987). The dimensions of the wedged-shaped conformation are such that it could easily penetrate deep into the major groove of the DNA with its tip pointing into the helix center. It is possible that a very similar folded conformation is adopted by CRA at the initial stages of the binding process, subsequently to be followed by further change in the relative orientation of the oligosaccharide side chains (e.g., the folding of sugar B), which provides for the locking of the drug in place.

Registry No. CRA, 7059-24-7; CRA-B, 113779-28-5; CRA-OAc, 6992-71-8.

References

Keniry, M. A., Brown, S. C., Berman, E., & Shafer, R. H. (1987) *Biochemistry 26*, 1058-1067.

Miyamoto, M., Kawamatsu, Y., Kawashima, K., Shinohara, M., Tanaka, K., Tatsuoka, S., & Nakanishi, K. (1967) *Tetrahedron 23*, 421-437.

Remers, W. A. (1979) in *The Chemistry of Antitumor Antibiotics*, Vol. 1, pp 133-175, Wiley, New York.

Scardale, J. N., Yu, R. K., & Prestegard, J. H. (1986) *J. Am. Chem. Soc. 108*, 6778-6784.

Thiem, Y., & Meyer, B. (1979) *J. Chem. Soc., Perkin Trans. 2*, 1331-1336.

Thiem, Y., & Meyer, B. (1981) *Tetrahedron 37*, 551-558.

Van Dyke, M. W., & Dervan, P. B. (1983) *Biochemistry 22*, 2372-2377.

Weinberger, S., Shafer, R. H., & Berman, E. (1988) *Biopolymers* (in press).

Solution Structure of the 45-Residue MgATP-Binding Peptide of Adenylate Kinase As Examined by 2-D NMR, FTIR, and CD Spectroscopy†

David C. Fry,‡,§ D. Michael Byler,‖ Heino Susi,‖ Eleanor M. Brown,‖ Stephen A. Kuby,⊥ and Albert S. Mildvan*,‡

Department of Biological Chemistry, The Johns Hopkins University School of Medicine, 725 North Wolfe Street, Baltimore, Maryland 21205, Eastern Regional Research Center of the U.S. Department of Agriculture, Philadelphia, Pennsylvania 19118, and Laboratory for the Study of Hereditary and Metabolic Diseases and Departments of Biological Chemistry and Medicine, University of Utah, Salt Lake City, Utah 84108

Received August 31, 1987; Revised Manuscript Received December 15, 1987

ABSTRACT: The structure of a synthetic peptide corresponding to residues 1-45 of rabbit muscle adenylate kinase has been studied in aqueous solution by two-dimensional NMR, FTIR, and CD spectroscopy. This peptide, which binds MgATP and is believed to represent most of the MgATP-binding site of the enzyme [Fry, D. C., Kuby, S. A., & Mildvan, A.S. (1985) *Biochemistry 24*, 4680-4694], appears to maintain a conformation similar to that of residues 1-45 in the X-ray structure of intact porcine adenylate kinase [Sachsenheimer, W., & Schulz, G. E. (1977) *J. Mol. Biol. 114*, 23-26], with 42% of the residues of the peptide showing NOEs indicative of ϕ and ψ angles corresponding to those found in the protein. The NMR studies suggest that the peptide is composed of two helical regions of residues 4-7 and 23-29, and three stretches of β-strand at residues 8-15, 30-32, and 35-40, yielding an overall secondary structure consisting of 24% α-helix, 38% β-structure, and 38% aperiodic. Although the resolution-enhanced amide I band of the peptide FTIR spectrum is broad and rather featureless, possibly due to disorder, it can be fit by using methods developed on well-characterized globular proteins. On this basis, the peptide consists of 35 ± 10% β-structure, 60 ± 12% turns and aperiodic structure, and not more than 10% α-helix. The CD spectrum is best fit by assuming the presence of at most 13% α-helix in the peptide, 24 ± 2% β-structure, and 66 ± 4% aperiodic. The inability of the high-frequency FTIR and CD methods to detect helices in the amount found by NMR may result from the short helical lengths as well as from static and dynamic disorder in the peptide. Upon binding of MgATP, numerous conformational changes in the backbone of the peptide are detected by NMR, with smaller alterations in the overall secondary structure as assessed by CD. Detailed assignments of resonances in the peptide spectrum and intermolecular NOEs between protons of bound MgATP and those of the peptide, as well as chemical shifts of peptide resonances induced by the binding of MgATP, are consistent with the previously proposed binding site for MgATP on adenylate kinase.

Adenylate kinase catalyzes the reaction

$$\text{MgATP} + \text{AMP} \rightleftharpoons \text{MgADP} + \text{ADP}$$

The enzyme contains two distinct nucleotide binding sites: the MgATP site, which binds MgATP and MgADP, and the AMP site, which is specific for AMP and uncomplexed ADP. We have recently examined the MgATP site in a series of NMR[1] studies on rabbit muscle adenylate kinase (Fry et al., 1985) and on a synthetic peptide, corresponding to residues 1-45 of the enzyme, that binds metal-ATP with comparable

† This work was supported by National Institutes of Health Grants DK28616 (to A.S.M.) and DK07824 (to S.A.K.).

‡ The Johns Hopkins University School of Medicine.

§ Present address: Department of Physical Chemistry, Hoffmann-La Roche, Inc., Nutley, NJ 07110.

‖ Eastern Regional Research Center of the U.S. Department of Agriculture.

⊥ University of Utah.

[1] Abbreviations: NMR, nuclear magnetic resonance; NOE, nuclear Overhauser effect; T_1, longitudinal relaxation time; Cr^{3+}ATP, β,γ-bidentate chromium adenosine triphosphate; FTIR, Fourier transform infrared; CD, circular dichroism; COSY, two-dimensional *J*-correlated NMR spectroscopy; NOESY, two-dimensional NOE NMR spectroscopy; RMS, root mean square; 2-D, two dimensional; DSS, sodium 4,4-dimethyl-4-silapentanesulfonate; A/D, analogue to digital; $d_{\alpha N}$, d_{NN}, and $d_{\beta N}$ (Wüthrich et al., 1984), short, NOE-producing distances between the NH proton of a given residue and, respectively, the CαH, NH, or CβH proton of its N-terminal neighbor.

0006-2960/88/0427-3588$01.50/0